

Archive ouverte UNIGE

https://archive-ouverte.unige.ch

Chapitre de livre 1990

Published version

Open Access

This is the published version of the publication, made available in accordance with the publisher's policy.

La Negra-Coquimbana manganiferous district, southern Atacama Desert, Chile

Pincheira, M.; Fontboté, Lluís

How to cite

PINCHEIRA, M., FONTBOTÉ, Lluís. La Negra-Coquimbana manganiferous district, southern Atacama Desert, Chile. In: Stratabound Ore Deposits in the Andes. Fontboté, L., Amstutz, G.C., Cardozo, M., Cedillo, E. & Frutos, J. (Eds.) (Ed.). Berlin: Springer, 1990. p. 365–378.

This publication URL: https://archive-ouverte.unige.ch/unige:78118

© This document is protected by copyright. Please refer to copyright holder(s) for terms of use.

La Negra-Coquimbana Manganiferous District, Southern Atacama Desert, Chile

M. PINCHEIRA^{1,2} and L. FONTBOTÉ^{2,3}

1 Introduction

The La Negra-Coquimbana (Mn-Fe) district is located in the Coastal Range of the southern Atacama desert, about 20 km northwest of Vallenar (28° 22'S. lat and 70° 31'W. lat; Fig. 1).

The deposits are mainly stratiform (locally called mantos) and appear in three main levels on the top of a volcano-sedimentary sequence of Lower Cretaceous age (Bandurrias Formation; Segerstrom 1960a). This formation has a wide extension in the Coastal Range of north Chile (27°–30°S.), and consists mainly of andesitic rocks with intercalations of sedimentary rocks of upper Valanginian to upper Barremian ages (Biese 1942; Corvalán 1955).

The mines in this area (La Negra, Porvenir, Coquimbana, and Venus), were exploited in this century at successive times especially during the first and second world war due to the high price of manganese. The ore extracted had a maximum Mn-grade of 46-48%.

2 Geologic Setting

In the La Negra-Coquimbana district (Coastal Range) rocks of the Bandurrias Formation and plutonic rocks of a batholitic complex of dioritic-tonalitic composition crop out. These units form a well-developed north-south-trending belt, which represents the remains of a magmatic arc of Lower Cretaceous age. Toward the east, in the Andean Range, a parallel belt of contemporaneous sedimentary rocks appears (Chañarcillo Group, Biese 1942; Corvalán 1955). All transitional environments between volcanic facies toward the west and marine sedimentary facies toward the east can be recognized. These units, as a whole, are interpreted as a magmatic arc-back-arc basin developed over continental crust (Abad 1977; Mercado 1979; Coira et al. 1982).

Stratabound ore deposits occur in different geotectonic positions of this pair as shown by Fontboté (this Vol.). A west-east zonation pattern of the stratabound ore deposits correlates well with geotectonic environments trending north-south, which are largely determined by the subduction mechanism in the west margin of

¹ Departamento de Geociencias Universidad de Concepción, Chile

² Mineralogisch-Petrographisches Institut der Universität, INF 236, D-6900 Heidelberg, FRG

³ Present address: Département de Minéralogie, 13, rue des Maraîchers, CH-1211 Genève 4, Switzerland

L. Fontboté, G.C. Amstutz, M. Cardozo,

E. Cedillo, J. Frutos (Eds.)

[©] Springer-Verlag Berlin Heidelberg 1990

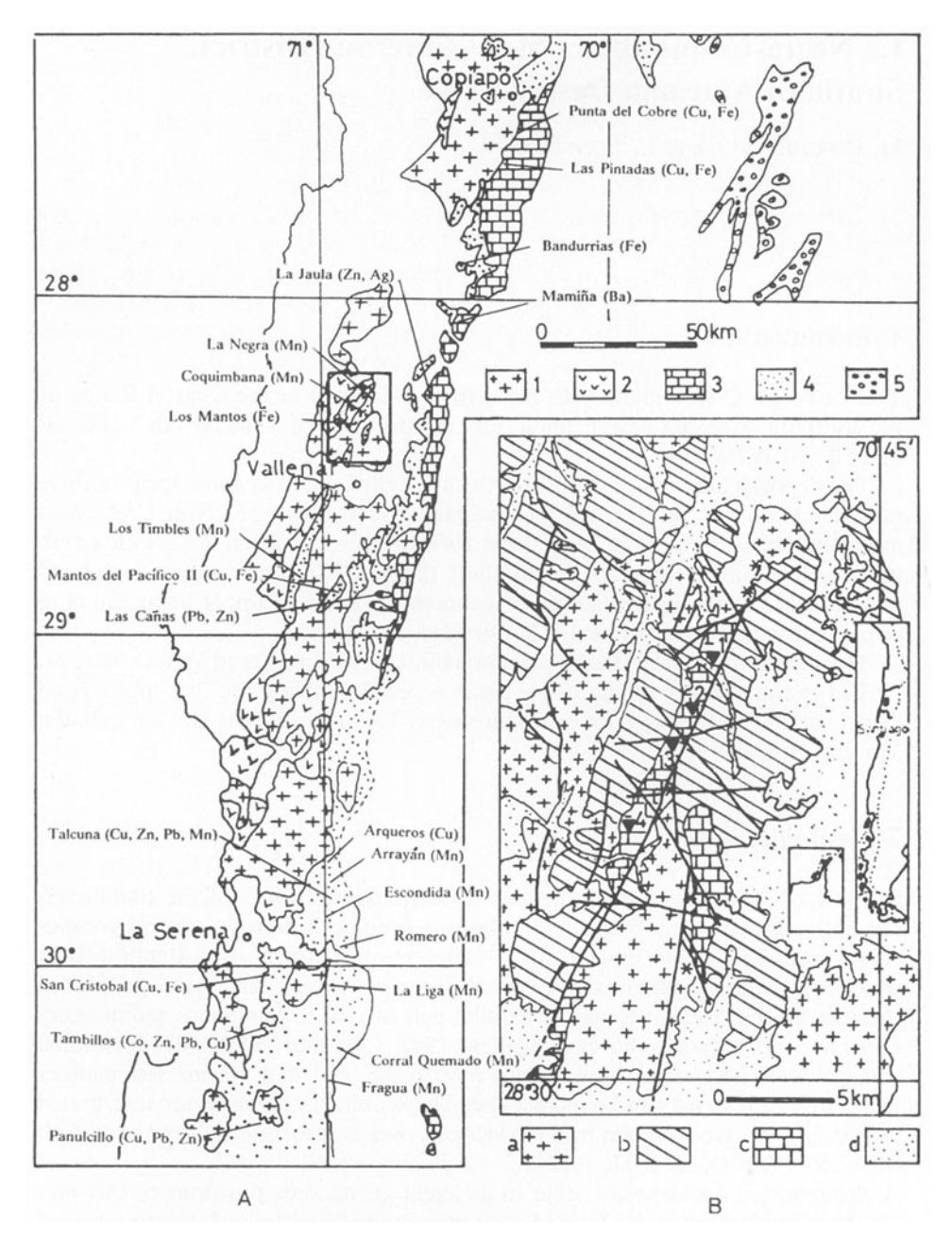


Fig. 1. A Stratabound ore deposits in the Lower Cretaceous units of the Atacama region (see also Cisternas this Vol.; Díaz this Vol.). I Coastal batholith; 2 volcanic facies; 4 transitional facies (volcanic rocks with intercalation of sedimentary rocks) of the Bandurrias Formation; 3 marine sedimentary facies (Chañarcillo Group); 5 red sandstones. B Geologic map of the district. I La Negra mine; 2 Porvenir mine; 3 Coquimbana mine; 4 Venus mine; * = tabular subvertical magnetite-ore-bodies a Dioritic-tonalitic rocks; b Andesitic rocks; c calcareous sedimentary rocks of the Bandurrias Formation; d modern sediments and terraces

the South American plate. In the La Negra-Coquimbana district, the hosting rocks were formed in a NNE-SSW-trending intra-arc basin, which extended parallel to the outcrops of the Lower Cretaceous magmatic arc (Pincheira and Thiele 1982). The Bandurrias Formation in this area is composed of andesitic lava flows, tuffs, and breccias, with some intercalations of sandstones, limestones, and chert. The Mn-Fe-rich layers are intercalated in chert and limestones, in the upper part of the sequence closely associated with tuffs and breccias. The sequence in the district is folded, dipping west, $60-80^{\circ}$ with a NNE strike. Mining works comprise open pits and underground works, as for example at the Coquimbana Mine, where they reach a depth of 130 m (Behncke 1944). On the surface these mantos extend continuously for 9 km. To the north, they are covered by Tertiary terraces; to the south and west, they are intruded by tonalitic rocks.

3 General Stratigraphy of the District

The Cretaceous sequence that appears in the La Negra-Coquimbana district can be subdivided into the following two sequences:

- A volcanic base (b-1, b-2), 1400 to 2500 m thick, consisting of andesitic rocks with a minor amount of rhyolitic intercalations. This sequence includes less than 10% of sedimentary rocks.
- An upper volcano-sedimentary sequence (a-1 to a-8), 700 m thick, composed of andesitic lava flows, tuffs, and breccias, with more than 30% of sedimentary intercalations consisting of calcareous sandstones, limestones and chert.

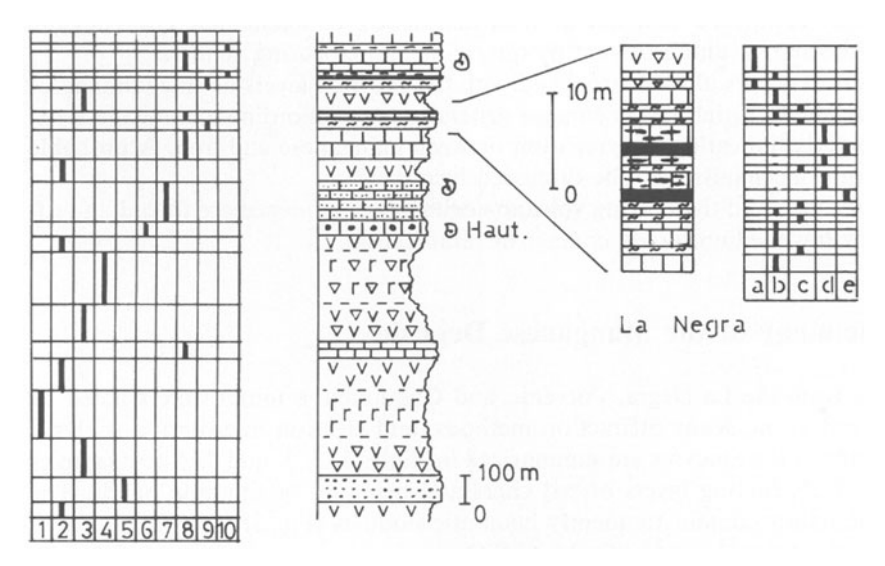


Fig. 2. Stratigraphic column of the district. I Rhyolites; 2 andesites; 3 andesitic breccias; 4 andesitic dacitic tuffs; 5 volcanic sandstones; 6 calcarenite; 7 sandy-limestones; 8 limestones; 9 ferruginous chert; 10 calcilutites; a andesitic breccias; b dark gray limestones; c ferruginous chert; d limestones with Fe-rich nodules; e Mn-mantos

The general stratigraphic column shows the following units from top to bottom (Fig. 2):

- a-1) 200 m of limestones with intercalations of greenish and reddish chert. Some hematitic layers (5 to 20 cm thick) are intercalated in the cherty strata:
- a-2) 70 m of greenish andesitic-dacitic tuffs and breccias, composed of fragments of andesites, fragments of Fe-rich sandstones, quartz and feldspar grains;
- a-3) 20 m of dark gray to red Mn-Fe-rich limestones with intercalations of ferruginous chert. This section contains the two main Mn-mantos in the district;
 - a-4) 150 m of brownish dark gray limestones;
 - a-5) 80 m of andesitic volcanic rocks, at the bottom with a minor intercalation of sandy tuffs;
 - a-6) 60 m of gravish limestones. Towards the bottom this section grades to sandy limestones:
- a-7) 90 m of greenish sandy-tuffs, composed of andesitic fragments and lenses of fine-grained hematite in a micritic matrix;
- a-8) 50 m of gray calcarenite, in beds 20 to 60 cm thick. They consist of intraclasts of micrite, cemented by microsparite. The detritic fraction is composed of fragments of andesites, tuffs, feldspar, and quartz:
- b-1) 1000 to 1800 m of andesitic lava flows, tuffs, and breccias with minor intercalations of limestones and volcanogenic sandstones in beds 20 cm to 1 m thick;
- b-2) 400 to 700 m of andesitic lava flows, tuffs, and breccias with a minor amount of rhyolitic intercalations.

4 Manganese Deposits

Several Mn-Fe-rich mantos can be recognized in the La Negra-Coquimbana district, but only two have been exploited. At the mines, the mantos dip almost vertically, with a NNE strike, and are concordant with the stratification. They generally contain several thin bands (5 to 20 cm) of manganese minerals, alternating with thin bands (2 to 5 cm) of red chert or limestones. The Mn-rich mantos have a massive texture composed of a fine-grained assemblage of oxide minerals. They are fractured, faulted, and cross-cut by quartz-hematite-bearing veinlets.

Hematite occurs always associated with the Mn-rich layers as fine laminae or nodules. The iron-rich layers contain generally only subordinate manganese oxides, possibly indicating a segregation between manganese and iron. A probable segregation mechanism will be discussed below.

The mantos and the hosting volcano-sedimentary sequence are folded and affected by low-medium grade contact metamorphism.

5 Mineralogy of the Manganese Deposits

Samples from the La Negra, Porvenir, and Coquimbana mines were studied by optical reflection, X-ray diffraction methods, and electron microprobe analysis. The results of the analyses are summarized in Tables 1, 2, 3, and 4. A few samples consist of alternating layers of red chert and hematite or limonite bands. The limonitic bands contain frequently hematitic nodules (Fig. 3).

Braunite 3(Mn³⁺, Fe³⁺)₂O₃.Mn²⁺ SiO₃ is the main ore mineral of the La Negra and Coquimbana Mines. Two chief fabrics are recognized: (a) layered granular aggregates (most common), where individual equant grains are packed tightly with only traces of gangue or secondary minerals along the grain boundaries

Table 1. Mineralogy of selected samples of the district (see also Table 5)

Sample	Description	Mineralogy
Porveni	r mine:	
P-7	Limonitic-hematitic layers	Hematite-andradite-goethite-chert. Hematite-quartz-goethite (veinlets)
Coquim	bana mine:	
P-1	Massive banded Mn-ore	Hausmannite- α -vredenburgite-pyrolusite- tephroite. Calcite (veins)
La Negr	ra mine:	
P-2	Massive banded Mn-ore	Franklinite-α-vredenburgite-pyrolusite-cryp tomelane-coronadite-manjiroite
P-3	Massive banded Mn-ore	Braunite-hausmannite-man- jiroite-pyrolusite-cryptomelane-spessartine
P-5	Massive banded Mn-ore with lamination of chert	Braunite-hausmannite-pyrolusite-birnessite. Calcite-quartz (veins)
P-17	Fe-rich nodules in laminated chert	Hematite-goethite-chert. Quartz-hematite (veinlets)

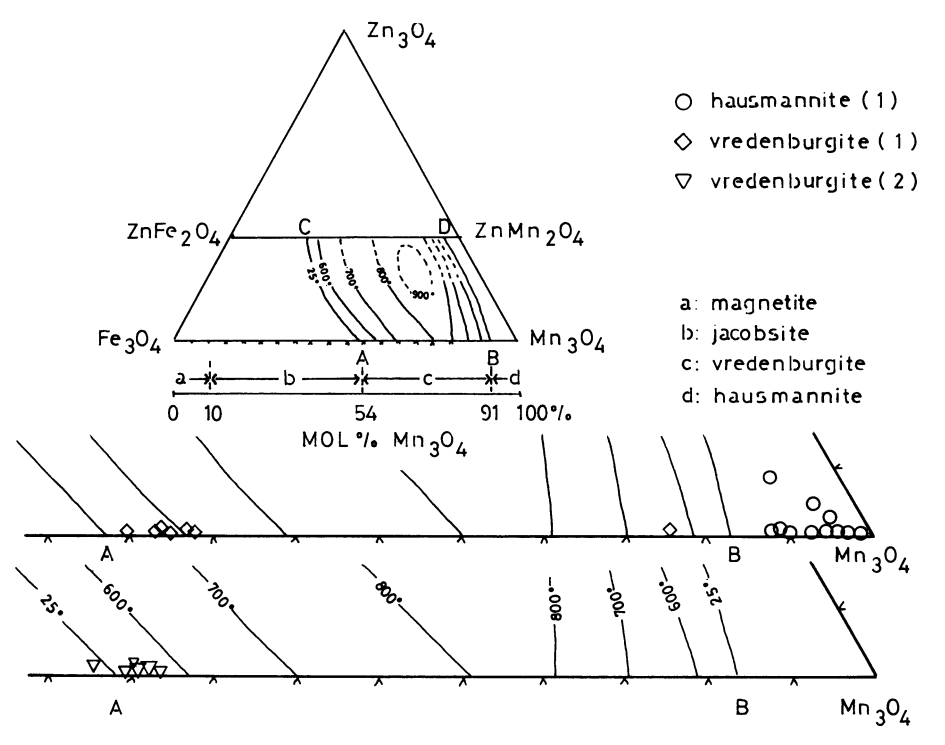


Fig. 3. The system Fe₃O₄-Mn₃O₄-ZnMn₂O₄-ZnFe₂O₄. Equilibrium diagram for the Zn-Mn-Fe spinels (Mason 1947), and composition of hausmannites from the Coquimbana mine. Electron microprobe analyses of La Coquimbana (1) and (2) of the La Negra mine. As the temperature rises the field of solid immiscibility (ABCD at room temperature) contracts and finally disappears between 900 and 1000 °C

	1	2	3	4	5	6
Mn_2O_3	73.07	79.00	79.21	67.24	65.81	61.93
MnO	10.49	9.62	9.39	29.05	31.59	32.51
CuO	n.d.	n.d.	n.d.	n.d.	n.d.	n.d.
ZnO	0.07	0.01	0.03	2.43	0.48	0.31
MgO	n.d.	n.d.	n.d.	n.d.	n.d.	n.d.
CaO	1.89	1.70	0.90	0.17	0.05	0.15
Na ₂ O	n.d.	n.d.	n.d.	n.d.	n.d.	n.d.
K ₂ O	0.08	n.d.	n.d.	n.d.	n.d.	n.d.
BaO	n.d.	n.d.	n.d.	n.d.	n.d.	n.d.
PbO	n.d.	n.d.	n.d.	n.d.	0.62	n.d.
Al_2O_3	1.83	0.43	0.89	0.92	1.04	1.05
Fe_2O_3	2.76	n.d.	n.d.	0.17	0.52	1.51
As_2O_3	n.d.	n.d.	n.d.	n.d.	n.d.	n.d.
V_2O_3	0.01	0.04	n.d.	n.d.	n.d.	n.d.
Cr_2O_3	n.d.	n.d.	n.d.	n.d.	n.d.	n.d.
SiO ₂	10.60	10.01	9.16	0.19	0.70	1.52
TiO_2	0.22	n.d.	0.07	n.d.	0.05	0.09
SO_3	n.d.	n.d.	n.d.	n.d.	n.d.	n.d.
Total	101.03	100.83	99.65	100.16	100.87	99.06
	3 number of		he basis of	12.000 oxyge	ens and 4, 5,	6 on the
	4.000 oxygens	s:				
Mn^{3+}	5.552	5.950	5.896	1.939	1.883	1.789
Mn ²⁺	0.887	0.806	0.777	0.932	1.006	1.045
Zn	0.005	0.001	0.002	0.068	0.013	0.008
Pb	_	_	_	_	0.006	_
Ca	0.206	0.179	0.090	0.006	0.001	0.006
Fe ³⁺	0.211	_	_	0.004	0.014	0.043
Al	0.219	0.049	0.098	0.041	0.046	0.047
Si	1.082	0.987	0.865	0.007	0.026	0.057
Ti	0.016	_	0.005	_	0.001	0.002

Total iron as Fe_2O_3 . The relative amounts of MnO and Mn_2O_3 were recalculated from total manganese assuming that the sum of the R^{3+} elements and Ti equals 6000 for braunite and equals 3000 for hausmannite.

and (b) isolated and well-crystallized braunite grains dispersed in a matrix of carbonates (sample P-3) or included in secondary manganese oxides (sample P-5). Between both fabric types a complete gradation is observed.

Hausmannite $(Mn^{2+}, Mn^{3+})_3O_4$ is abundant and widespread at the La Coquimbana Mine. It occurs mainly as granular and massive aggregates forming well stratified bands, and also as nodular and lenticular structures surrounded by rims of silicates. Hausmannite is usually intergrown with α -vredenburgite (Mason 1943) and is associated with silicates (largely tephroite) which fill the interstitial

^a (1), (2) and (3) braunite of the La Negra mine: (1) massive banded ore; (2) and (3) core of isolated euhedral grains in a carbonated matrix. (4), (5) and (6) hausmannite of the La Coquimbana mine: (4) micro veinlet of hausmannite; (5) massive banded ore; (6) nodule.

Table 3. Electron microprobe analyses of alpha-vredenburgite^a

	1	2	3	4	5
Mn ₂ O ₃	11.90	20.44	24.60	20.36	18.26
Fe ₂ O ₃	42.89	40.75	40.78	42.96	44.55
MnO	35.90	33.02	30.00	31.45	32.67
CuO	n.d.	0.02	n.d.	n.d.	n.d.
ZnO	0.38	0.45	0.27	0.57	0.45
MgO	0.37	0.05	n.d.	0.49	0.28
CaO	0.32	0.75	0.31	0.14	0.12
Na ₂ O	n.d.	n.d.	n.d.	n.d.	0.08
K ₂ O	0.06	n.d.	0.05	n.d.	n.d.
BaO	n.d.	n.d.	n.d.	n.d.	n.d.
PbO	n.d.	n.d.	n.d.	n.d.	n.d.
Al_2O_3	3.01	1.52	0.73	2.03	1.46
As_2O_3	n.d.	n.d.	n.d.	n.d.	n.d.
V_2O_3	n.d.	n.d.	n.d.	n.d.	n.d.
Cr_2O_3	n.d.	n.d.	n.d.	n.d.	n.d.
SiO ₂	4.33	2.23	1.09	n.d.	0.49
TiO_2	0.33	0.47	0.53	1.89	1.99
SO_3	n.d.	n.d.	n.d.	n.d.	n.d.
Total	99.50	99.68	98.36	99.90	100.38
Number o	of cations on	the basis of 4	.000 oxygens	s:	
Mn ³⁺	0.355	0.585	0.723	0.584	0.523
Fe ³⁺	1.195	1.153	1.185	1.218	1.262
Mn ²⁺	1.125	1.052	0.981	1.004	1.041
Ca	0.013	0.030	0.012	0.005	0.004
Mg	0.020	0.002	_	0.027	0.015
Zn	0.010	0.012	0.007	0.016	0.012
Al	0.131	0.067	0.033	0.090	0.065
Si	0.160	0.083	0.042	_	0.018
Ti	0.009	0.013	0.015	0.053	0.056

Total iron as Fe_2O_3 . The relative amount of Mn_2O_3 was recalculated from total manganese assuming that the sum of the cations equals 3.000.

space between grains. In the sample P-1 from the La Coquimbana Mine, a thin veinlet of hausmannite cuts the microlayers of hausmannite, α -vredenburgite, and Mn-bearing silicates.

Alpha-vredenburgite (Mn^{2+} , Fe^{2+} , Mg, Zn)(Fe^{3+} , Mn^{3+}) $_2O_4$ a metastable phase within the two exsolved phases region of the system Fe_3O_4 - Mn_3O_4 (Mason 1947; Van Hook and Keith 1958) occurs at the La Coquimbana and La Negra Mines as fine-layered 0.1-3 mm thick aggregates with only minor interstitial silicates or secondary manganese oxides. Under the microscope appears one phase with weak bireflection, low to medium anisotropy, and reflectivity similar to braunite. At the Coquimbana Mine alternating bands of hausmannite+tephroite and α -vredenburgite were observed.

and α -vredenburgite were observed. Franklinite (Zn, Fe²⁺, Mn²⁺)(Fe³⁺, Mn³⁺)₂O₄ was indentified only by X-ray diffraction methods and occurs probably intergrown with α -vredenburgite, both minerals having similar optical properties.

^a Laminated layers of α -vredenburgite: (1), (2), (3) from La Coquimbana Mine and (4), (5), from La Negra Mine.

Table 4. Electron microprobe analyses of secondary Mn-oxides of the La Negra mine a

	1	2	3	4	5	6	7
MnO ₂	87.68	89.40	89.88	96.53	94,75	85.78	70.40
MnO	n.d.	n.d.	n.d.	n.d.	n.d.	3.45	3.27
CuO	n.d.	0.06	0.03	n.d.	n.d.	0.04	n.d.
ZnO	0.33	0.11	n.d.	n.d.	n.d.	n.d.	0.09
MgO	1.40	0.37	0.47	0.10	n.d.	n.d.	n.d.
CaO	1.67	1.14	1.75	0.27	0.29	1.19	0.21
Na ₂ O	2.41	2.54	1.49	0.24	n.d.	1.45	n.d.
K_2O	0.12	0.64	0.32	0.68	0.48	5.14	n.d.
BaO	0.56	0.50	0.08	n.d.	n.d.	n.d.	n.d.
PbO	0.04	0.34	0.06	n.d.	n.d.	n.d.	12.58
Al_2O_3	0.41	1.11	1.02	0.64	0.71	0.79	0.56
Fe ₂ O ₃	0.09	n.d.	n.d.	n.d.	n.d.	n.d.	n.d.
As_2O_3	n.d.	n.d.	0.13	n.d.	0.17	n.d.	0.90
V_2O_3	0.06	n.d.	0.01	n.d.	n.d.	0.03	0.09
Cr ₂ O ₃	n.d.	0.63	0.04	0.04	n.d.	0.02	n.d.
SiO ₂	0.80	1.09	0.37	0.38	0.55	0.33	0.80
TiO_2	n.d.	n.d.	n.d.	0.05	n.d.	n.d.	n.d.
SO ₃	n.d.	0.14	n.d.	0.07	n.d.	0.36	n.d.
H ₂ O#	(4.42)	(1.93)	(4.33)	(0.99)	(3.05)	(1.39)	(11.11)
Total	100.00	100.00	100.00	100.00	100.00	100.00	100.00

basis of 2.000 oxygens:

4 .							
*Mn ⁴⁺	7.336	7.415	7.497	0.957	0.966	7.321	7.320
*Mn ²⁺	_	0.064	_	_	_	0.361	0.416
*Cu	_	0.006	0.002	_		_	_
*Zn	0.029	0.009	_	_	-		0.010
Pb	0.001	0.011	0.002	_	-	_	0.509
*Mg	0.253	0.066	0.085	0.002	-	_	_
*Ca	0.216	0.146	0.225	0.004	0.004	0.157	0.033
Ba	0.026	0.023	0.004	_	-	_	_
Na	0.566	0.591	0.349	0.006	-	0.348	_
K	0.019	0.098	0.049	0.012	0.009	0.811	_
*Al	0.058	0.156	0.145	0.010	0.012	0.115	0.099
*Fe ³⁺	0.008	_	_	_	-	_	_
*Si	0.097	0.130	0.044	0.005	0.008	0.040	0.120
*Ti	_	-	_	_	-	_	_

Total iron as Fe₂O₃. The total amounts of MnO and MnO₂ were recalculated from total manganese assuming that the sum of the cations (*) equals 8.000, except for pyrolusite, where it equals 1.000. (#) H₂O calculated from difference to 100%.

Manjiroite (Na, K)₁₋₂(Mn⁺², Mn⁺⁴)₈O₁₆.xH₂O was observed only at the La Negra Mine. It shows three predominant fabrics: fine cryptocrystalline monomineralic aggregates forming well-defined layers (1-5 mm thick), a matrix of isolated euhedral crystals of braunite, and disseminated in the matrix associated with pyrolusite and gangue silicates. Manjiroite is also cross-cut by veinlets of pyrolusitecryptomelane and occurs also subordinated in pyrolusite-coronadite-rich nodules.

^a Massive banded manjiroite (1), (2) and (3); (4), (5) pyrolusite and (6) cryptomelane filling a cavity; (7) coronadite intergrowths with pyrolusite in nodules.

Pyrolusite (MnO₂) occurs in pores as microcrystalline aggregates within braunite, hausmannite, and α -vredenburgite, or associated with manjiroite and cryptomelane in the matrix or as veinlets. Braunite and hausmannite are replaced by pyrolusite, cryptomelane, and birnessite along fractures and cleavage, while α -vredenburgite exhibits no supergene alteration. Some of the fractures and veinlets are filled with calcite.

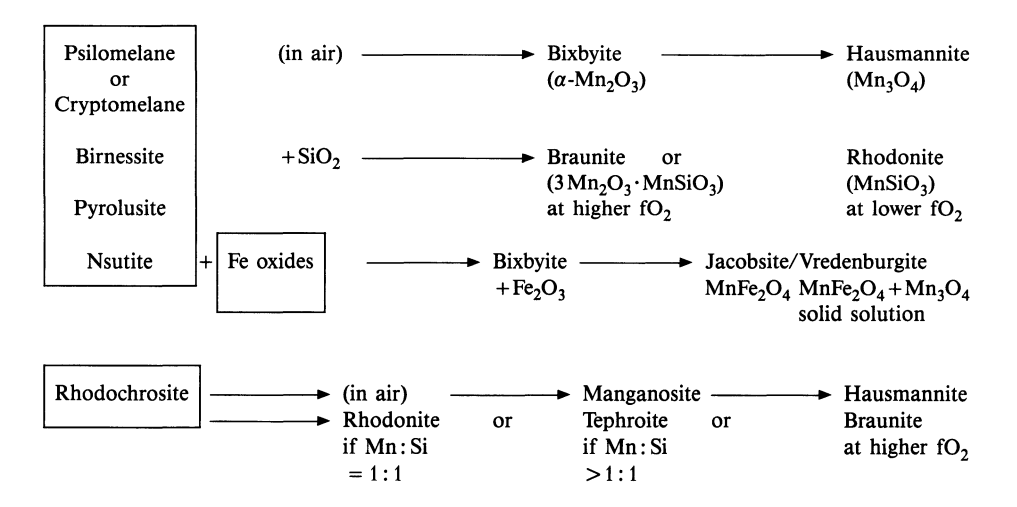
6 Discussion

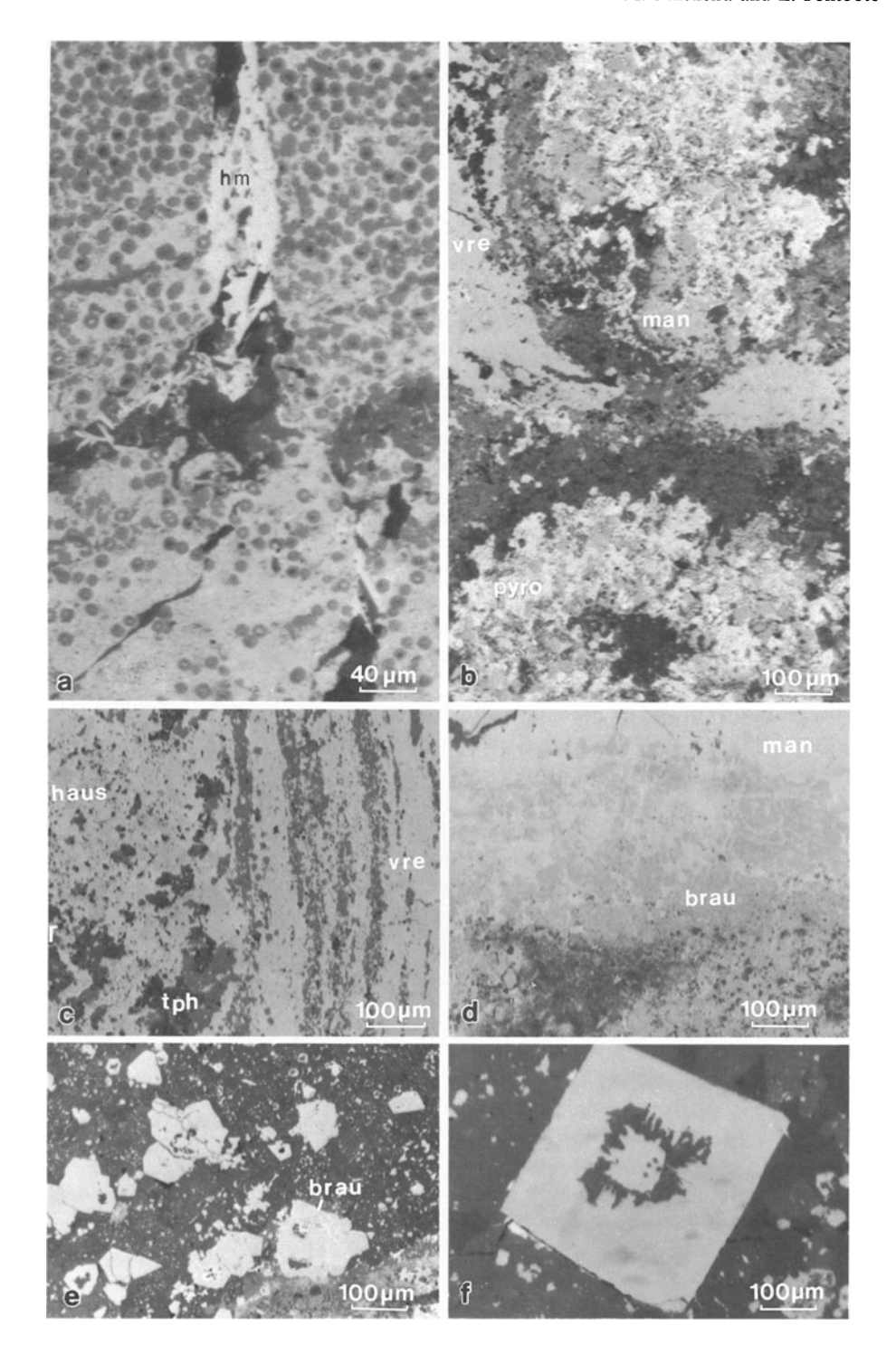
Hausmannite, jacobsite/vredenburgite, and braunite occur widely as metamorphic ore (de Villiers 1960; Huebner 1967; Watanabe et al. 1970; Roy 1973; Frenzel 1980). In addition, hausmannite, vredenburgite, and braunite had been synthesized in the laboratory at a relatively high temperature (Mason 1947; Van Hook and Keith 1958; Muan 1959a, b; in Bonatti et al. 1976), and are commonly found in deposits affected by green schist-facies metamorphism. The presence of α -vredenburgite in samples of the two mines indicates, according to the equilibrium diagram for the system Fe₃O₄-Mn₃O₄-ZnMn₂O₄-ZnFe₂O₄ (Mason 1947), a maximum temperature of formation of about 600 °C (Fig. 3).

The natural occurrences suggest the following sequence of stability of phases in the Mn-Si system with increasing temperature (Roy 1973):

Hariya (1961) found that todorokite samples heated in air at a temperature of 560 °C for 1 h produced an X-ray pattern containing lines of hausmannite. Birnessite also changed to hausmannite at 560 °C. The Hariya test with manganite, MnO(OH), resulted in the production of pyrolusite at 300 to 360 °C, bixbyite at 580 °C, but hausmannite was not produced when the sample was heated to 1050 °C. Groutite, MnO(OH), produced also bixbyite and hausmannite at comparable temperatures.

The lack of braunite, jacobsite, and hausmannite in modern nodules and metalliferous sediments from ocean basins and shallow seas (e.g., Barents Sea, Gulf of Maine, Kara Sea; Roy 1981) suggests that the natural conditions on the





sea floor are not favorable to the formation of these minerals in sedimentary environments (Sorem and Gunn 1967; Bonatti et al. 1976; Rona 1978; Toth 1980). Modern studies of metalliferous sediments from the ocean basins indicate that the common iron and manganese compounds that occur as nodules or crusts on active spreading centers and seamounts consist of poorly crystallized oxides and hydroxide phases. These may be manganites, birnessite, todorokite, and rhodochrosite in the Mn-rich crust (Bonatti et al. 1976), or goethite and nontronite in iron-rich crusts (Toth 1980).

Lithology, textural features, and form of the orebodies are consistent with a synsedimentary formation within an intra-arc basin (Pincheira and Thiele 1982). In this environment volcanic-exhalative influence is very likely and could explain the stratiform geometry of the deposits, textural features as lamination of chert, and carbonates alternating with Mn-Fe-rich layers.

It is reasonable to assume that recrystallization during diagenesis and subsequent contact metamorphism of primary, poorly crystallized Mn-Fe phases could result in conversion to a braunite-hausmannite- α -vredenburgite-tephroite-spessartine assemblage with relict sedimentary textures, such as those occurring in the La Negra-Coquimbana district.

The separation of manganese from iron probably resulted from the following process:

a) oxidation and precipitation of iron in subsurface hydrothermal conduits of Mn-Fe-bearing solutions due to the lower solubility of Fe³⁺. The resultant Fe-depleted-Mn-rich solution may precipitate at the surface close to the exhalative zone.

This hypothesis agrees with the geologic frame of the district (see Fig. 1), where important subvertical tabular magnetite orebodies (Ménard 1988) occur along a north-south-trending fault zone close to the stratiform ore deposits.

b) after deposition, segregation by diagenetic processes could take place by selective mobilization and concentration of manganese by low Eh pore-space waters (Strakhov 1966; Krauskopf 1957). Thus, first Mn⁴⁺ and Mn³⁺, and then Fe³⁺ are reduced. Under these condition iron will be the last element to be reduced (and rendered mobile) and the first one to be oxidized (and rendered immobile). Manganese tends to move ahead all the time. It remains in solution and precipitates later. Thus, a progressive segregation of the two elements takes place. Perhaps this process is responsible of the formation of hematite layers from Mn-Fe rich sediments.

Fig. 4. Microplates of the La Negra-Coquimbana district. a) Andradite garnet cemented by fine grains of hematite, cross-cut by a quartz-hematite (hm) veinlet (P-7, Porvenir mine, reflected light, parallel Nic.); b) α -vredenburgite (vre) and pyrolusite (pyro)-manjiroite (man)-rich nodules surrounded by a rim of silicates (P-2, la Negra mine, reflected light, parallel Nic.); c) α -vredenburgite (vre), hausmannite (haus) and tephroite (tph) microbands (P-1, La Coquimbana mine, reflected light, parallel NIC.); d) microbands of braunite (brau) and manjiroite (man) (P-5, La Negra mine, reflected light, parallel Nic.); e) euhedral crystals of braunite (brau) partially replaced by pyrolusite in a matrix of carbonates (P-3, La Negra mine, reflected light, parallel Nic.); f) detail of an euhedral crystal of braunite (P-3, La Negra mine, reflected light, parallel Nic.)

	Deposition	Diagenesis	Metamorphism	Sup. Alt.
Hematite I			,	
Hematite II				_
Goethite				
Chert				
Hausmannite				•
Tephroite				•
α -vredenburgite				-
Pyrolusite	• • • • • • • • • • • • • • • • • • • •	• • • • • • • • • • • • • • • • • • • •		
Cryptomelane		• • • • • • • • • • • • • • • • • • • •		
Manjiroite	• • • • • • • • • • • • • • • • • • • •	• • • • • • • • • • • • • • • • • • • •		
Franklinite				-
Braunite				-
Birnessite	• • • • • • • • • • • • • • • • • • • •	• • • • • • • • • • • • • • • • • • • •		
Coronadite	• • • • • • • • • • • • • • • • • • • •	• • • • • • • • • • • • • • • • • • • •		
Andradite				
Spessartin				-
Calcite		• • • • • • • • • • • • • • • • • • • •		

Table 5. Paragenetic position of the mineral assemblages

Braunite, α -vredenburgite, and hausmannite probably are formed because of post-depositional reactions, as a result of lower-medium contact metamorphism affecting the host sequence of the mantos. The metamorphism was produced by intrusion of Lower Cretaceous tonalitic rocks of the magmatic-arc in the volcanosedimentary cover.

The occurrence of pyrolusite, cryptomelane, manjiroite, and birnessite replacing trivalent or divalent manganese-oxides, is related to supergene alteration processes (Table 5).

7 Conclusions

A genetic model considering exhalative and diagenetic processes is postulated for the formation of the La Negra-Coquimbana district. The model can be summarized as follows:

- 1. Discharge of hydrothermal solutions through the sea floor may provide silica and amorphous Mn and Fe hydroxide phases, which precipitate as hydrated colloids to form Mn-Fe-rich sediments.
- 2. Fractionation at several geologic environments of iron and manganese due to the lower solubility of iron compounds led to Fe-rich and Mn-rich bodies.
- 3. Metamorphism related to Lower Cretaceous intrusions caused recrystallization and formation of braunite-hausmannite- α -vredenburgite-tephroite-franklinite-spessartin assemblages.
- 4. Supergene alteration processes after the decreasing temperature of the system provided conditions for partial replacement of hausmannite and braunite by pyrolusite, manjiroite, cryptomelane, and birnessite.

The metal-bearing hydrothermal solutions were probably related to contemporaneous volcanic activity, perhaps producing mobilization of metals from tuffs and andesitic lava flows by circulation of sub-sea floor hydrothermal convection systems close to the exhalative centers, in a way similar to that proposed among others by Bonatti et al. (1976) and Rona (1978) in modern deposits from oceanic spreading zones.

Acknowledgments. This work was completed while the first author held an academic exchange scholarship from the Deutscher Akademischer Austauschdienst (DAAD) at the Mineralogical-Petrological Institute, University of Heidelberg. We are also grateful to the Deutsche Forschungsgemeinschaft (DFG) which support this project, in collaboration with the Universidad de Concepción in Chile. The manuscript has benefited from critical reading by G. Frenzel (Heidelberg); R.A. Zimmerman corrected the English text.

References

Abad E (1977) Acerca de la paleogeografía neocomiana en la región al sur de Copiapó, provincia de Atacama. Chile. Assoc Geol Argentina 32 (1):24-33

Behncke R (1944) Estudio de los yacimientos de manganeso de Carrizal. Provincia de Atacama, Chile. Mem de Título, Univ Chile

Biese W (1942) La Distribución del Cretácico Inferior al sur de Copiapó. I Congr Panam Ing Min Geol 1 (2):429-466

Bonatti E, Zerbi M, Kay R, Rydell H (1976) Metalliferous deposits from the Apennine ophiolites: Mesozoic equivalents of modern deposits from oceanic spreading centers. Geol Soc Am Bull 87:83-94, 9 figs

Cisternas ME, The Bandurrias iron deposit, Atacama Region, northern Chile. This Vol, pp 505-512 Coira B, Davidson J, Mpodozis C, Ramos V (1982) Tectonic and magmatic evolution of the Andes of Northern Argentina and Chile. Earth Sci Rev 18:303-332

Corvalán J (1955) El sistéma Cretáceo de la provincia de Atacama, 19 p (ined)

Das Gupta DR (1965) Oriented transformation of manganite during heat treatment. Min Mag 35:131-139

de Villiers JPR (1960) The manganese deposits of the Union of South Africa. Geol Surv South Africa, Handbook 2, 271 p

Díaz L, The Bellavista Zn-Ag mine, Copiapó region, Chile. This Vol, pp 513-522

Fontboté L, Stratabound ore deposits in the Central Andes: A review and a classification according to their geotectonic setting. This Vol, pp 79-110

Frenzel G (1980) The manganese ore minerals. In: Varentsov IM, Grasselly G (eds) Geology and geochemistry of manganese. Schweizerbart, Stuttgart 1:25-158

Frondel C, Klein C (1965) Exsolution in franklinite. Am Mineral 50:1671 - 1680

Hariya Yu (1961) Mineralogical studies on manganese dioxide and hydroxide minerals in Hokkaido, Japan: J Fac Sci Hokkaido Univ Ser 4, Geol Min 10:641-702

Huebner JS (1967) Stability relations of minerals in the system Mn-Si-C-O. Ph. D. Thesis, Johns Hopkins University, Baltimore, Maryland

Krauskopf KB (1957) Separation of manganese from iron in sedimentary processes: Geochem Cosmochim Acta 12:61-84

Mason B (1943) Alpha-vredenburgite. Geol Foren Forhandl 65:263-272

Mason B (1947) Mineralogical aspect of the system $Fe_3O_4-Mn_3O_4-ZnMn_2O_4-ZnFe_2O_4$. Am Mineral 32:426-441

Muan A (1959) Phase equilibria in the system manganese oxide-SiO₂ in air. Am J Sci 257:297-315 Ménard JJ (1988) Les relations volcanisme, plutonisme et minéralisation dans la ceinture de fer du Chili: La région d'El Algarrobo. These Docteur D'état, Univ Paris-Sud, D'Orsay

Mercado M (1979) Recientes progresos del conocimiento geológico en la región de Atacama Chile. II Congr Geol Chile 1:A25-A44

Pincheira M (1981) Geología de la mitad oriental del Cuadrángulo Astillas. Nuevos antecedentes de la franja ferrífera principal entre los 28° 15'y 28° 30' S. Mem Título, Univ Chile, 263 p (unpublished)

Pincheira M, Thiele R (1982) El Neocomiano de la Cordillera de la Costa al NW de Vallenar (28° 15' a 28° 30' L.S.). Situación tectónica del borde occidental de la cuenca marina neocomiana trasarco. III Congr Geol Chile III Actas 1:A236-A261 Concepción, Chile

Rona P (1978) Criteria for recognition of hydrothermal mineral deposits in oceanic crust. Econ Geol 73 (2):135 – 160

Roy S (1968) Mineralogy of the different genetic types of manganese deposits. Econ Geol 63:760 – 786 Roys S (1973) Genetic studies on the Precambrian manganese formations of India with particular references to the effects of metamorphism. In: Genesis of Precambrian Iron and Manganese Deposits. Proc Kiev Symp UNESCO, Paris, Earth Sci Ser 9:229 – 242

Roy S (1981) Manganese deposits. Academic Press, London, 458 p

Segerstrom K (1960) Cuadrángulo Quebrada Paipote, provincia de Atacama. Inst Inv Geol Chile 2 (1), 33 p

Sorem R, Gunn D (1967) Mineralogy of manganese deposits, Olympic Peninsula. Wahington. Econ Geol 62:22-56

Stanton RL (1972) Ore petrology. Mc Graw-Hill, New-York, 713 p

Strakhov MN (1966) Types of manganese accumulation in present day basins: their significance in understanding of manganese mineralisation. Int Geol Rev 8:1172-1196

Toth J (1980) Deposition of submarine crusts rich in manganese and iron. Geol Soc Am Bull Part 1 91:44-54, 7 figs, 2 tables

Van Hook HJ, Keith ML (1958) The system Fe₃O₄-Mn₃O₄. Am Mineral 43:69-83

Watanabe T, Yui S, Kato A (1970) Metamorphosed bedded manganese deposits of the Noda-Tamagawa mine. In: Tatsumi T (ed) Volcanism and ore genesis. Univ Tokio Press, pp 143-152